AAAI26_W1_W3PHIAI-26_12

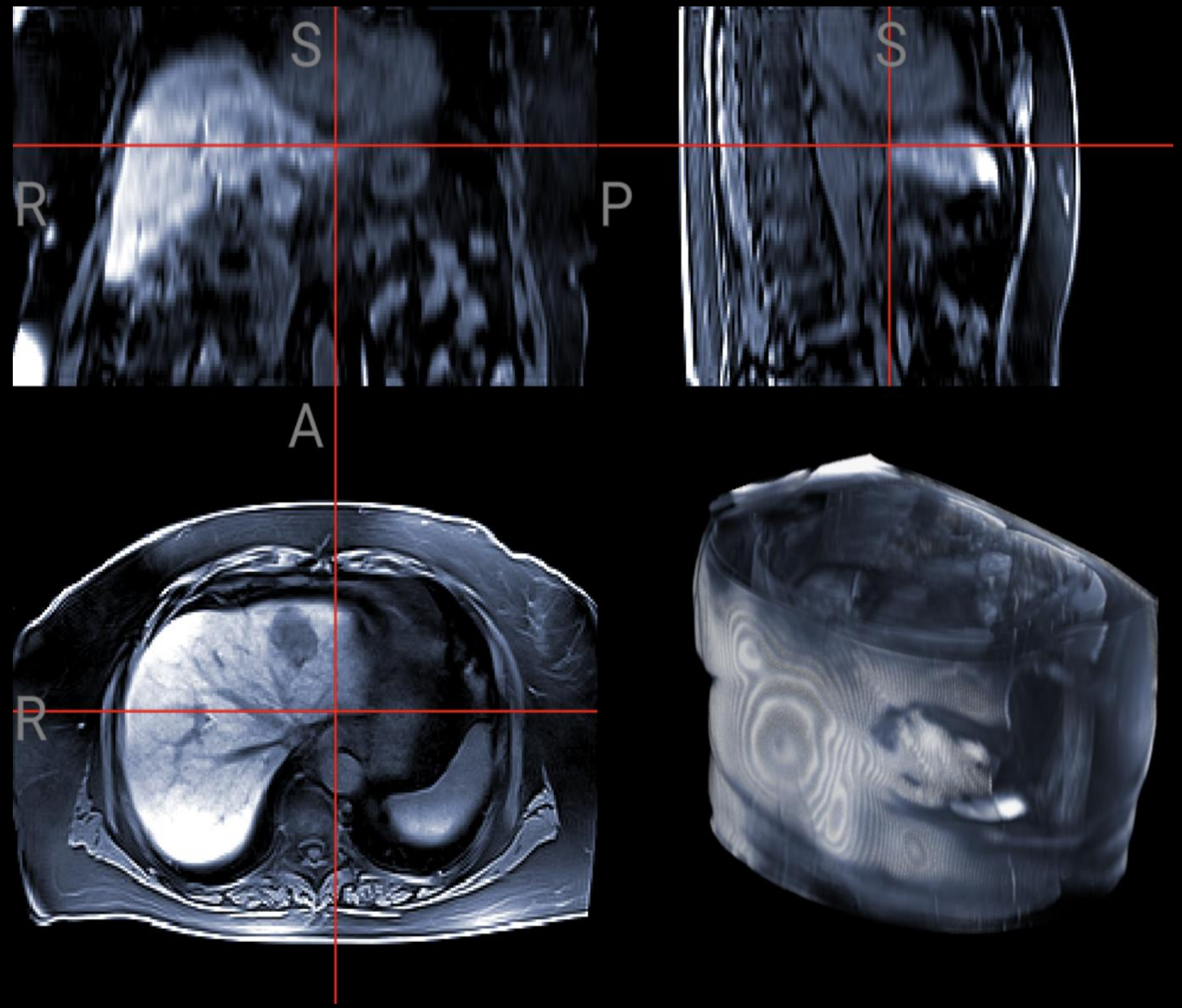

NeoNet:

An End-to-End MRI-Based Deep Learning Framework for Non-Invasive Prediction of Perineural Invasion

PRESENTER | MINKYUNG CHA

- Authors: Youngung Han, Minkyung Cha, Kyeonghun Kim, Induk Um, Myeongbin Sho, Joo Young Bae, Jaewon Jung, Jung Hyeok Park, Seojun Lee, Nam-Joon Kim, Woo Kyoung Jeong, Won Jae Lee, Pa Hong, KenYing-Kai Liao, Hyuk-Jae Lee

서울대학교 SEOUL NATIONAL UNIVERSITY

Seoul National University | Republic of Korea

CORE MESSAGE

1. Background and the Need for Study

Minimizing the need for invasive procedures in clinical diagnosis

-one of the key goals of medical imaging

+

time consuming, labor intensive, uncertain features and inter-observer variability…

Bottleneck of Conventional Radiological Interpretation

⇓

Need for Early, Noninvasive Identification of Subtle Prognostic Indicators

2. Perineural Invasion and the Clinical Paradox

PNI(Perineural Invasion):

infiltration of tumor cells along the nerves and their surrounding tissue
facilitated by active biochemical crosstalk - independent route of metastasis, potential cause of recurrence after surgery

/

Preoperative Identification of PNI aids Decisions surrounding Clinical Interventions.

However,

Definitive Identification of PNI Relies Exclusively on Preoperative Histopathology.

/

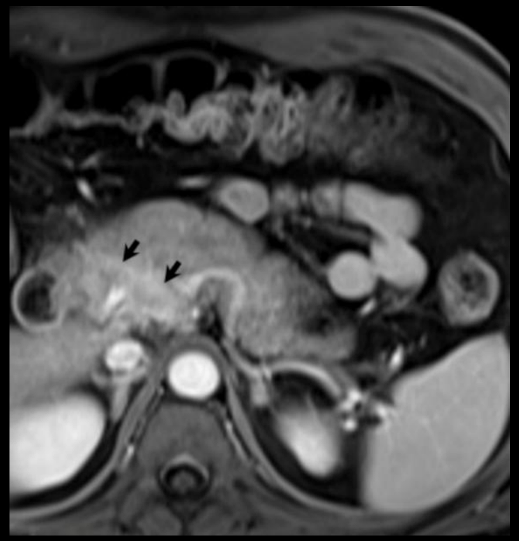

cues of perineural invasion in MRI

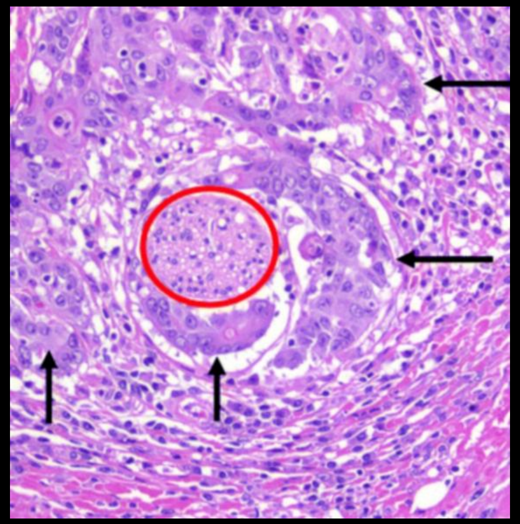

cues of perineural invasion in histopathology

Madhusudhan, K. S. (2021, September 1). Perineural invasion in gallbladder cancer. Letters to the Editor. Radiographics. https://doi.org/10.1148/rg.2021200222Tu, W., Gottumukkala, R. V., Schieda, N., Lavallée, L., Adam, B. A., & Silverman, S. G. (2023, June 15). Perineural invasion and spread in common abdominopelvic diseases: Imaging diagnosis and clinical significance.

3. Need for an End-to-End, MRI-based Diagnostic Model

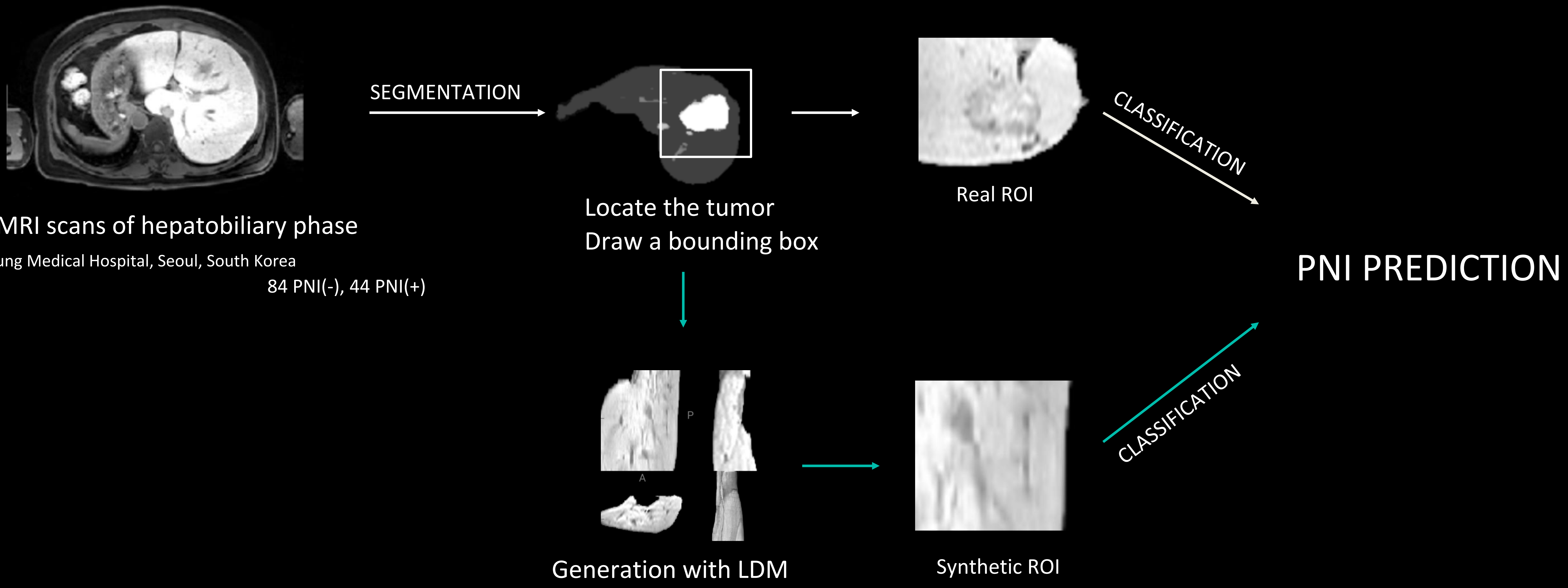

Training Step

3. Need for an End-to-End, MRI-based Diagnostic Model

YES,
THE TUMOR HAS INVADED THE NERVE.

INPUT MRI IMAGE

SEGMENTATION, TUMOR LOCALIZATION, ROI GENERATION, FINAL SUMMARY

PNI PREDICTION

NO,
THE NEURAL TISSUE IS INTACT.

In Actual Use

NEONET: TOTAL PIPELINE

NeoSeg | automated tumor ⇔ liver segmentation

NeoGen | generation of synthetic data based on extracted patches

NeoCls | trained with synthetic + real patches, final identification of PNI

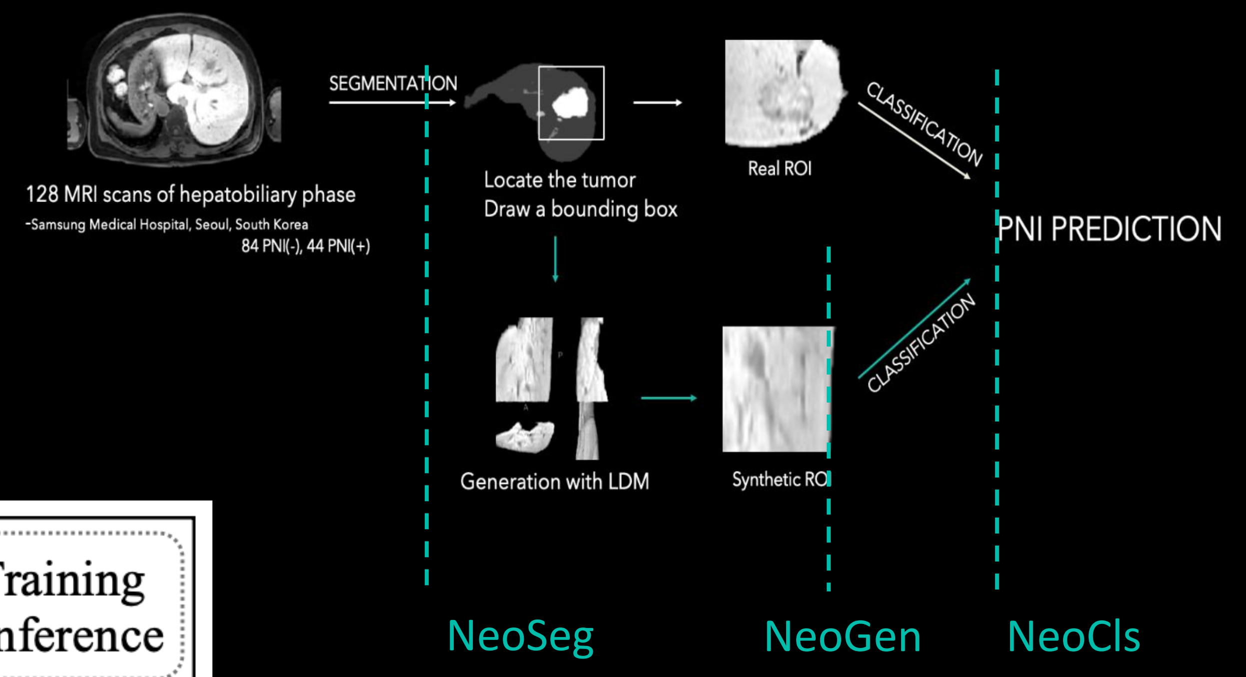

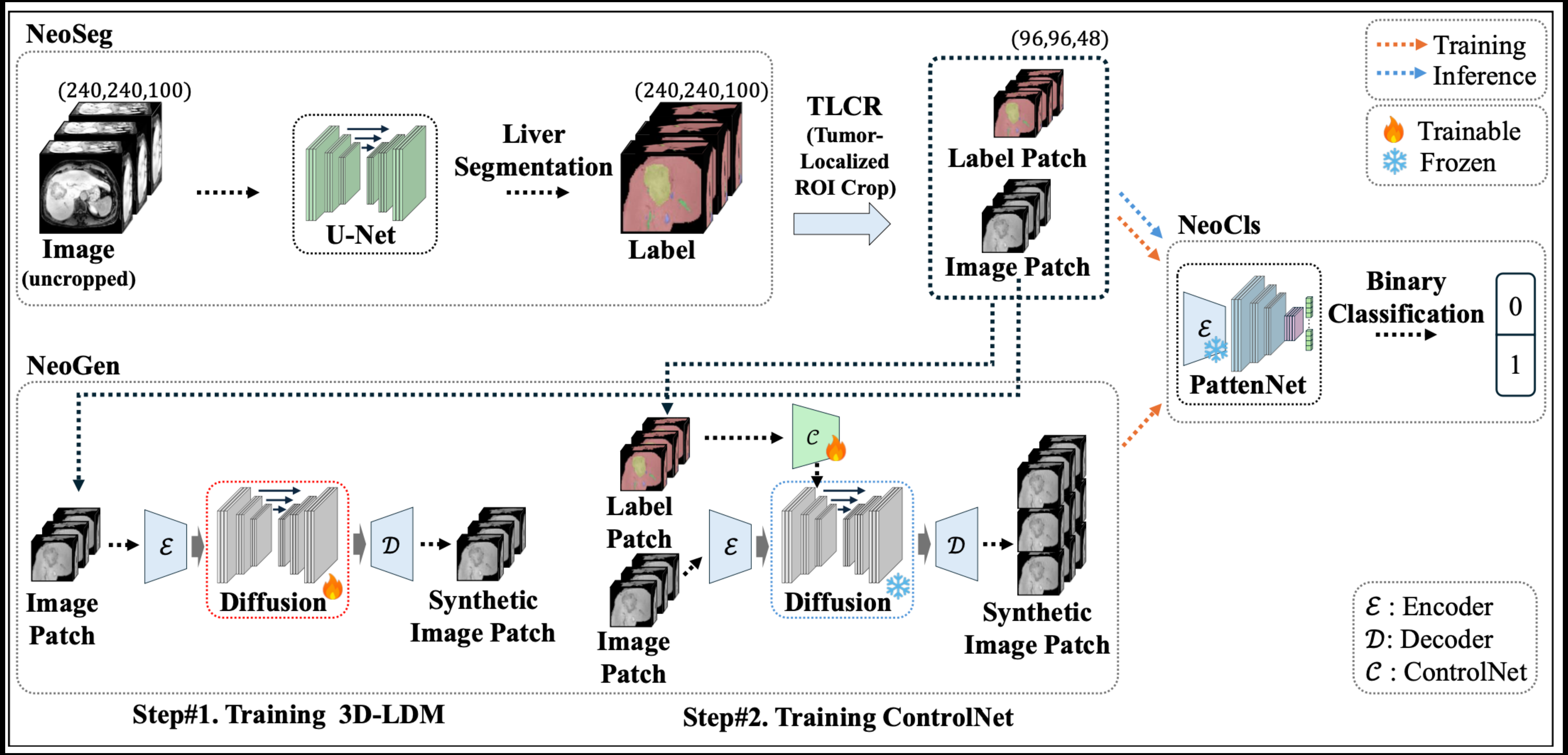

1. NeoSeg | SEGMENTATION AND TUMOR PATCH LOCALIZATION

Pretrained Baseline Models

Model	Mean Dice
U-Net	0.9453
SegResNet	0.9416
DynUNet	0.9482
SwinUNETR	**0.9516**

=>

TLCR

tumor centered crop on ROI

OUTCOME:
LOCALIZATION OF VALID FEATURES IN & AROUND THE TUMOR

Channel 1 | peritumoral region
Channel 2 | localized tumor core

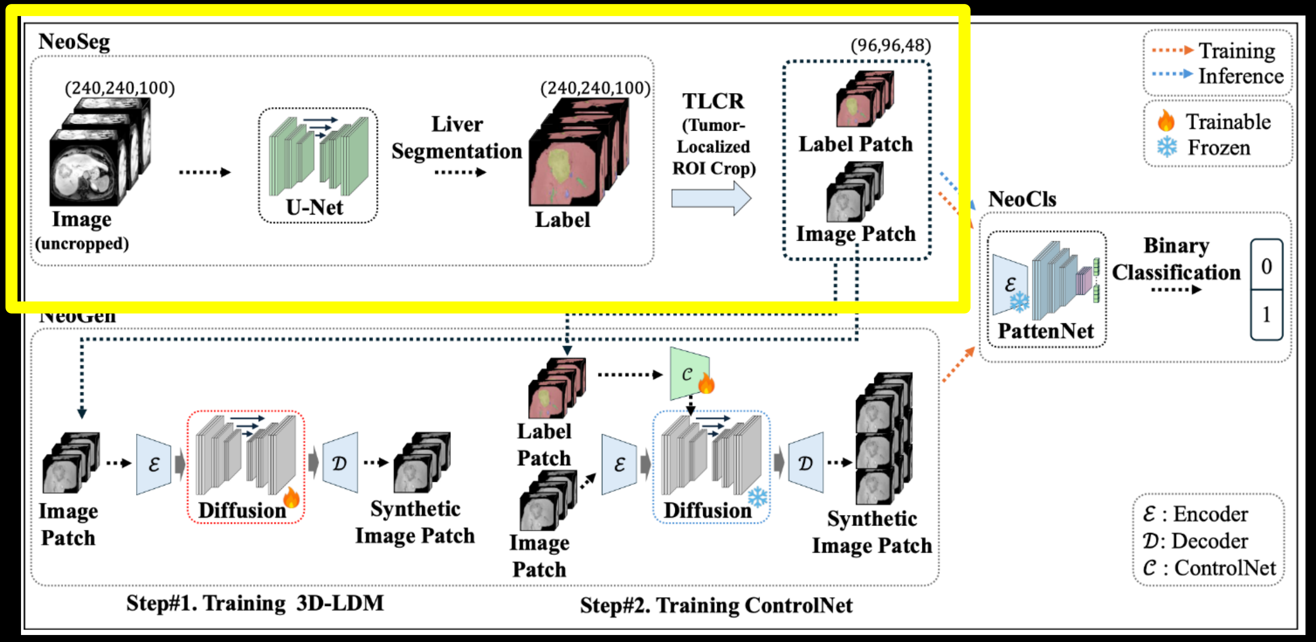

LOCALIZED MRI PATCH

OUTPUT OF NEOSEG

Input:
3D medical image $\mathbf{I}$, Crop size $\mathbf{C} = (c_x, c_y, c_z)$
Label map $\mathbf{L} = \{0 : \text{background},\ 1 : \text{liver},\ 2 : \text{tumor}\}$

Output:
Cropped vectors $\mathbf{T_1} \in \mathbb{R}^{c_x \times c_y \times c_z}$ (peritumoral mask)
and $\mathbf{T_2} \in \mathbb{R}^{c_x \times c_y \times c_z}$ (tumor mask)

1. Find tumor voxel coordinates:
$\mathcal{S} \leftarrow \{(x, y, z) \mid \mathbf{L}[x, y, z] = 2\}$

2. Check for empty tumor mask:
if $\mathcal{S}$ is empty **then**
$\mathbf{T_1}, \mathbf{T_2} \leftarrow \mathbf{0}^{c_x \times c_y \times c_z}$
return $\mathbf{T_1}, \mathbf{T_2}$

3. Calculate bounding box:
$[x_{\min}, y_{\min}, z_{\min}] \leftarrow \min(\mathcal{S})$
$[x_{\max}, y_{\max}, z_{\max}] \leftarrow \max(\mathcal{S}) + 1$

4. Determine Center & Crop region:
$\text{center} \leftarrow \left(\left\lfloor \frac{x_{\min}+x_{\max}}{2} \right\rfloor, \left\lfloor \frac{y_{\min}+y_{\max}}{2} \right\rfloor, \left\lfloor \frac{z_{\min}+z_{\max}}{2} \right\rfloor\right)$
$\text{start} \leftarrow \max\left(\text{center} - \frac{\mathbf{C}}{2}, 0\right)$
$\text{end} \leftarrow \text{start} + \mathbf{C}$

5. Extract and Generate Masks:
$\mathbf{I}_{crop} \leftarrow \mathbf{I}[\text{start} : \text{end}]$, $\mathbf{L}_{crop} \leftarrow \mathbf{L}[\text{start} : \text{end}]$
$\mathbf{T_1} \leftarrow \mathbf{I}_{crop}[\mathbf{L}_{crop} \in \{1, 2\}]$
$\mathbf{T_2} \leftarrow \mathbf{I}_{crop}[\mathbf{L}_{crop} \in \{2\}]$

return $\mathbf{T_1}, \mathbf{T_2}$

2. NeoGen | GENERATION OF SYNTHETIC MRI PATCH FOR TRAINING STAGE

3D Latent Diffusion Model (LDM)

$$\mathcal{L}_{LDM} = \mathbb{E}_{\mathcal{E}(x),\epsilon\sim\mathcal{N}(0,1),t}[||\epsilon - \epsilon_\theta(z_t,t)||_2^2]$$

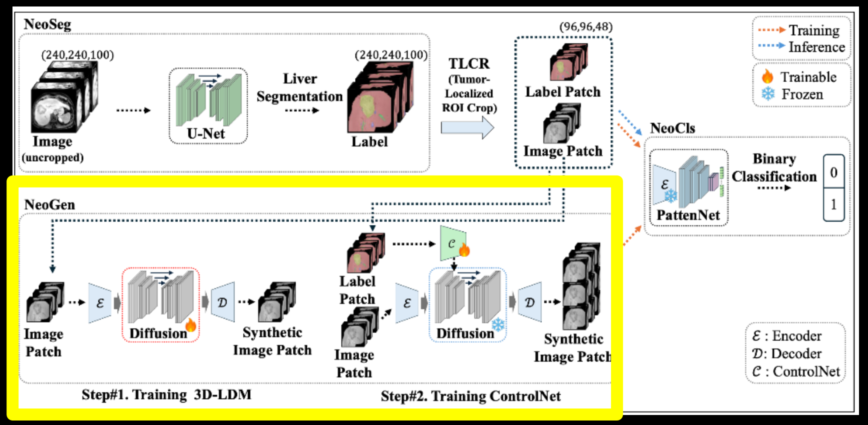

TRAINABLE COPIES OF LDM BLOCKS

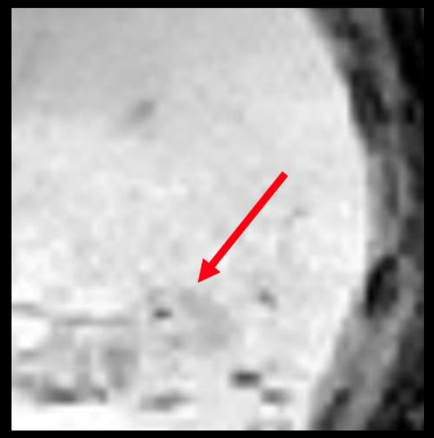

ROI EXTRACTED FROM THE PREVIOUS STAGE (NeoCls)

ControlNet-guided synthetic data generation

$$\mathbf{y}_c = F(\mathbf{x};\theta) + Z_2\left(F(\mathbf{x}+Z_1(\mathbf{c});\theta')\right)$$

$$\mathcal{L} = \mathbb{E}_{\mathbf{z}_0,\mathbf{c},\epsilon,t}\left[\|\epsilon - \epsilon_\theta(\mathbf{z}_t,t,\mathbf{c})\|_2^2\right]$$

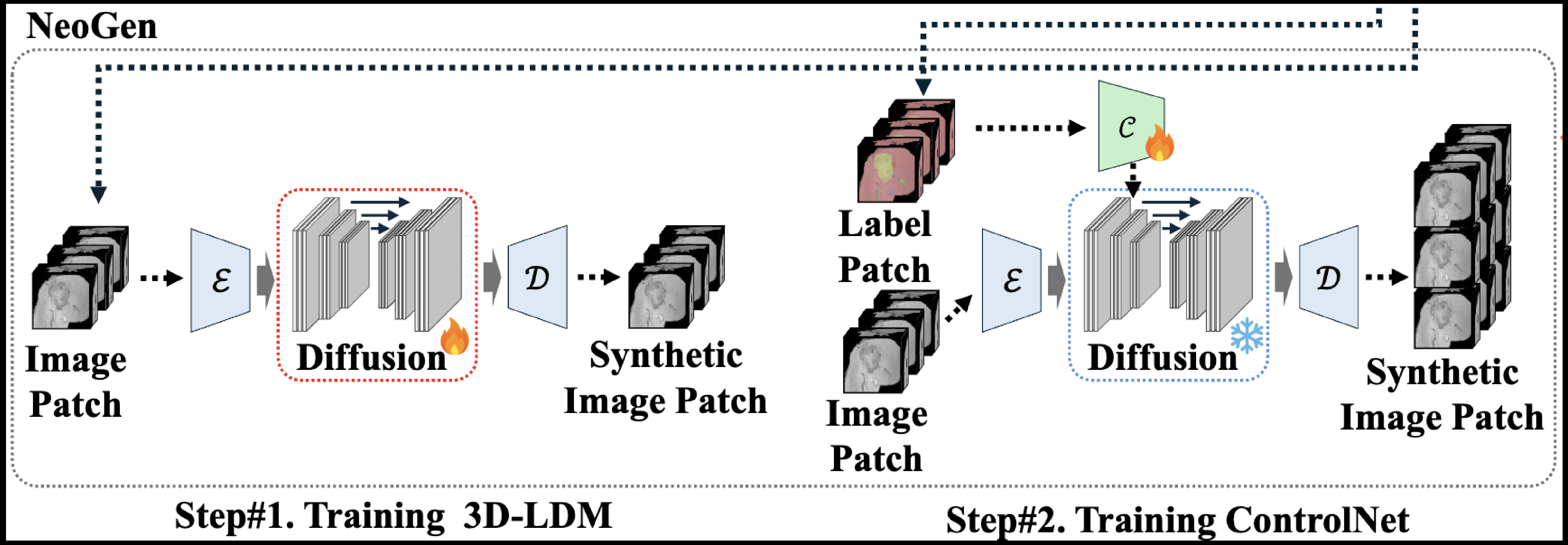

CLINICAL IMAGE

GENERATED IMAGE

OUTPUT OF NEOGEN

3. NeoCls | FINAL CLASSIFICATION STAGE

PattenNet: trained with synthetic + real patches, final identification of PNI

Frozen encoder from the prev.stage => Dual Attention block (DAB)

1) Channel Attention | dual channel of tumor / peritumoral region
2) Spatial Attention | localization on actual pni features

OUTPUT OF NEOCLS:
Binary Classification of PNI

Input sequence

$$\mathbf{F} \in \mathbb{R}^{D\times H\times W\times C}$$

Channel Attention

$$\mathbf{M}_c(\mathbf{F}) = \sigma(\mathrm{MLP}(\mathrm{AvgPool}(\mathbf{F})) + \mathrm{MLP}(\mathrm{MaxPool}(\mathbf{F})))$$

+

Spatial Attention

$$\mathbf{M}_s(\mathbf{F}) = \sigma(f^{7\times7\times7}([\mathrm{AvgPool}_c(\mathbf{F}); \mathrm{MaxPool}_c(\mathbf{F})]))$$

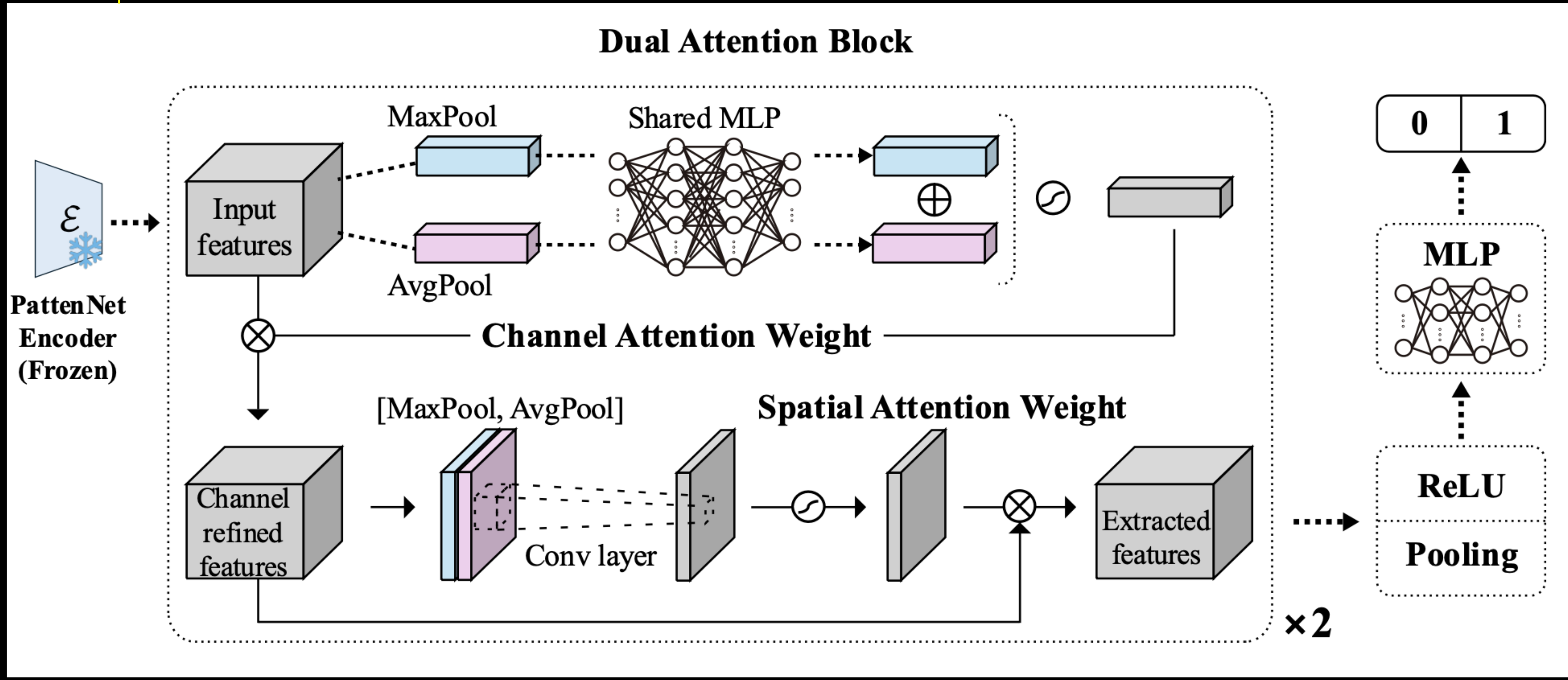

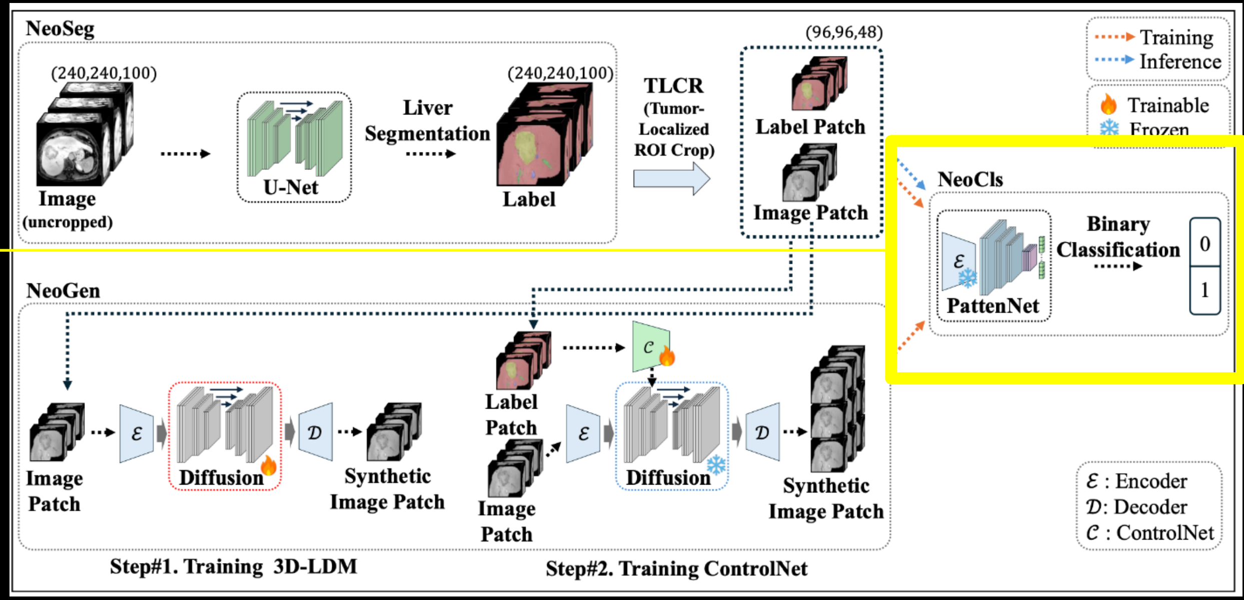

FINAL RESULT

COMPARATIVE ANALYSIS OF BASELINE MODELS ON AREA UNDER THE CURVE

Model (3D)	R (Imbalanced)	R + S (25%)	R + S (50%)	R + S (75%)	R + S (100% Balanced)
ResNet-50	0.6938	0.7388	0.7599	0.7551	0.7618
ResNet-101	0.6284	0.6989	0.7024	0.7117	0.7203
ResNet-152	**0.7078**	0.7233	0.7421	0.7382	0.7526
ResNet-200	0.6687	0.7250	0.7307	0.7397	0.7412
DenseNet-121	0.6788	0.7443	0.7380	0.7490	0.7551
DenseNet-169	0.6725	0.7021	0.7387	0.7434	0.7584
DenseNet-201	0.6911	0.7133	0.7226	0.7278	0.7311
DenseNet-264	0.6712	0.6899	0.7012	0.7037	0.7155
EfficientNet-B0	0.6798	0.6897	0.6995	0.6910	0.6998
EfficientNet-B1	0.6725	0.7127	0.7098	0.7101	0.7186
EfficientNet-B2	0.6623	0.6899	0.7085	0.7024	0.7110
EfficientNet-B3	0.6533	0.7215	0.7462	0.7671	0.7755
SwinTransformer	0.6829	0.7423	0.7454	0.7503	0.7522
PattenNet (Ours)	0.7001	**0.7577**	**0.7670**	**0.7812**	**0.7903**
Mean AUC	0.6760	0.7178	0.7294	0.7336	0.7417

*R: Real clinical data provided from the hostpital | S: synthetic data generated by NeoCls

CONSTITUENT ANALYSIS OF NEOCLS(PATTENNET) ARCHITECTURE

Configuration	AUC (R+S)
PattenNet (Full Model, 2 DABs)	**0.7903**
DAB Component Ablation (2 Blocks)	
w/ Channel Attention only	0.7276
w/ Spatial Attention only	0.7410
Number of DABs	
0 Blocks (Base LDM Encoder)	0.7001
1 Block	0.7589
3 Blocks	0.7713

CONCLUSION

LIMITATIONS

1. Data scarcity and Bias
   1-1. single center cohort
   1-2. small amount of data – total 128
   => uncertainty of generalization

2. Focused on relatively small portion of the field
   2-1. tumoral invasion around the 'nerve' only
   2-2. modality was restricted on HBP_MRI

FUTURE DIRECTIONS

NeoNetV2 - Towards a generalizable, noninvasive, diagnostic model on characteristics of neoplasm
Training on additional data & various modalities

AAAI26_W1_W3PHIAI-26_12

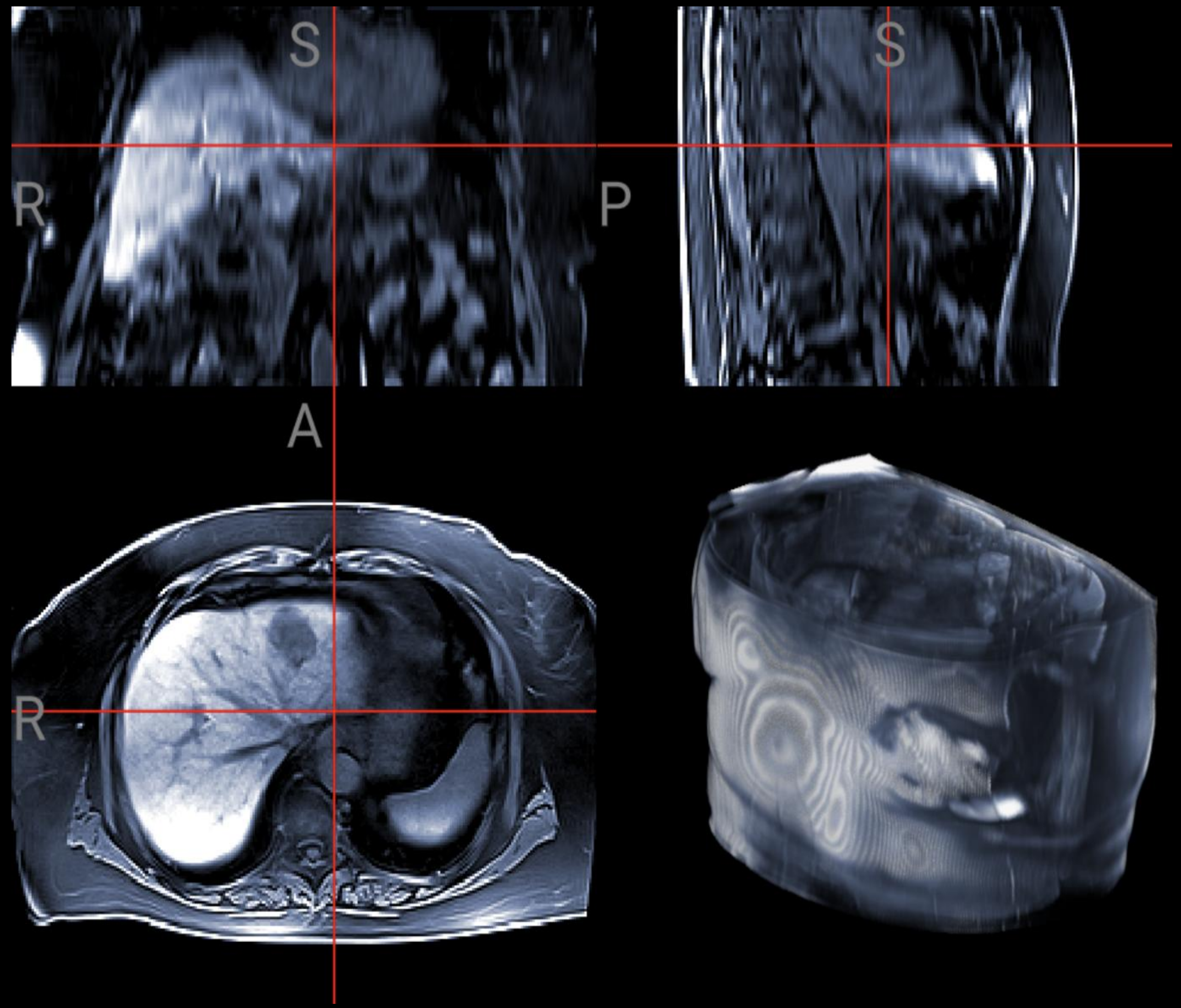

NeoNet:

An End-to-End MRI-Based Deep Learning Framework for Non-Invasive Prediction of Perineural Invasion

THANK YOU

Youngung Han, Minkyung Cha, Kyeonghun Kim, Induk Um, Myeongbin Sho, Joo Young Bae, Jaewon Jung, Jung Hyeok Park, Seojun Lee, Nam-Joon Kim, Woo Kyoung Jeong, Won Jae Lee, Pa Hong, KenYing-Kai Liao, Hyuk-Jae Lee

PRESENTER | MINKYUNG CHA

Seoul National University | Republic of Korea

서울대학교
SEOUL NATIONAL UNIVERSITY